Z-Pole Running for SiD

The SiD Consortium

DRAFT
November 7, 2016

Abstract

The ILC detectors will need extensive calibration and alignment, much of which will rely on physics data. The ultimate statistical precision achievable is likely to depend primarily on the number of well-measured charged tracks incident on specific detector elements. It has been suggested that it will be advantageous (or even necessary) to have significant ILC running at $\sqrt{s} = 91$ GeV to take advantage of the Z-pole cross section enhancement, even if the accelerator can only provide a much-reduced luminosity.

This preliminary study examines the expected charged particle fluxes from all processes at $\sqrt{s} = 91$ GeV and 500 GeV as a function of polar angle and momentum in the transverse plane. It is found that the ratio of the 500 GeV flux to that at the Z-pole has only a weak dependence on transverse momentum and is smallest when perpendicular to the beamline, rapidly rising in the forward regions. Even in the most central region, however, the lower cross section at high energies will be largely compensated by the expected higher luminosity. It therefore appears that there is no advantage in taking data at the Z-pole unless the luminosity is significantly higher than that currently forseen.

1 Introduction

The physics reach of the SiD detector at the ILC depends critically on the calibration and alignment of the different subdetectors. In particular, tracking elements will need to be aligned to an accuracy of microns (vertex detector), tens of microns (tracker) or hundreds of microns (muon detectors), and calorimeters will need calibrating to achieve a jet energy resolution at the few percent level.

The detailed calibration and alignment strategies for SiD will depend on the final detector technologies, and studies have just barely started. They will inevitably require a combination of detailed survey data, real-time monitoring and physics data from collisions (and possibly even cosmic rays and beam backgrounds).

The physics collision data available for these purposes will depend on the integrated luminosity delivered, the cross sections of the physics processes, and the kinematic distributions of the particles produced.

The ILC will deliver physics collisions at an energy of 250 GeV and above, with luminosities of the order of 10^{34} cm^{-2}s^{-1}. As described in the March 2016 paper from the ILC Parameters Joint Working Group, it should also be possible

(although far from trivial) to reconfigure the accelerator and beam delivery system to deliver collisions at the Z-pole, but with a relative drop in instantaneous luminosity of two orders of magnitude [2]. In this document we will take a first look at whether sacrificing some proportion of high-energy running to take data at the Z-pole offers an advantage for calibration and alignment purposes.

2 Energy Calibration

The ILC calorimeters are designed to use particle flow algorithms, in which the energy resolution depends on identifying the energy deposits from each incident particle. In the case of charged particles, these will be matched to tracks and the momentum of the track will be used to determine the energy of the particle for all except the highest energies (well above the Z-pole).

It is therefore likely that the calibration of the calorimeters will be performed at the particle level, and so the statistical precision of the collision data-dependent calibration will depend on the flux of charged particles at a given energy.

3 Tracking Alignment

The relatively straightforward requirements for muon detector alignment will probably be primarily achieved by external monitoring systems and are not expected to drive the data requirements. The vertex detector and main tracker alignment, on the other hand, will rely heavily on a statistically significant number of well-reconstructed tracks to achieve the required precision.

4 Charged Particle Fluxes

We have established that the statistical precision of calibration and alignment is likely to be driven by the charged particle flux. This will be lowest in the barrel region and at large radius. We therefore study the flux as a function of θ for values of p_T that are appropriate for calibrating the outer barrel tracking layer and ECAL. This will allow the direct determination of the number of tracks per 10 cm×10 cm module in this layer, and a good estimate of the flux into the calorimeter.

The radius of curvature of the trajectory of a charged particle in a magnetic field B is proportional to p_T/B where p_T is the particle's momentum in the plane transverse to the field. For a magnetic field of 5 T, a particle with the same charge as an electron or a proton with $p_T = 1$ GeV has a radius of curvature of 0.67 m, just sufficient to reach the inner layer of the ECAL barrel at 1.265 m.

4.1 Physics Processes

The cross section for the process

$$e^+ e^- \to Z^0 \to f\overline{f}$$

at high energy is reduced by three orders of magnitude when compared to the Z-pole. Taking into account the expected luminosity, this results in a rule of

thumb of about 30:1 for the number of on-pole events at high energy for equal running time.

Additional processes become important at high energy. These include the s-channel processes like

$$e^+e^- \rightarrow W^+W^-,$$

as well as t-channel processes like

$$e^+e^- \rightarrow ZZ.$$

In addition, photon–electron and photon–photon interactions have significant cross sections that lead to decays with charged particles of considerable p_T. The list of processes considered includes the full range of 1- through 4- and 6-fermion interactions, in addition to $\gamma\gamma$ production of 2- and 4-fermion events from beamstrahlung photons.

It should be noted that these processes lead to significant cross sections of W and Z bosons, summarized in Table 1.

Process	cross section (fb)
$e^+\gamma \rightarrow W\nu$	1200
$e^+\gamma \rightarrow Ze^+$	7600
$\gamma\gamma \rightarrow W^+W^-$	12
$e^+e^- \rightarrow Ze^+e^-$	4200
$e^+e^- \rightarrow eW\nu$	6400
$e^+e^- \rightarrow Z\gamma$	8200

Table 1: Dominant sources of heavy gauge bosons in photoproduction at a 500 GeV ILC

4.2 Results

Figure 1 shows the ratio of total charged particle fluxes at 500 GeV to that at the Z pole *at the same luminosity*. The left hand plot shows this ratio only for particles with $E > 1$ GeV, just sufficient to reach the outer tracking layer and ECAL at high angles. A more conservative selection is to require $E > 2$ GeV, as shown in the right hand plot, as tracks close to 1 GeV have a high angle of incidence giving large tracker clusters and poor penetration into the calorimeters.

At higher energies, more of the production is forward and the 500 GeV flux per unit luminosity is larger for most of the endcap region. In the central region, the flux at high energies is lower than at the Z-pole, but even requiring $E > 2$ GeV the reduction at $\theta \approx 90^\circ$ is not significantly larger than 100.

Figure 2 shows how the ratio depends on the minimum track p_T that is required. Note that this is not integrated over the polar angle, but rather in a slice around $\cos\theta = 0$ in the central barrel.

The total numbers of charged particles per fb^{-1} integrated over all polar angles, with $p_T > 1$ GeV are 6.56×10^8 with an average of 10.8 tracks per event at 91 GeV, and 7.92×10^6 with an average of 2.6 tracks per event at 500 GeV.
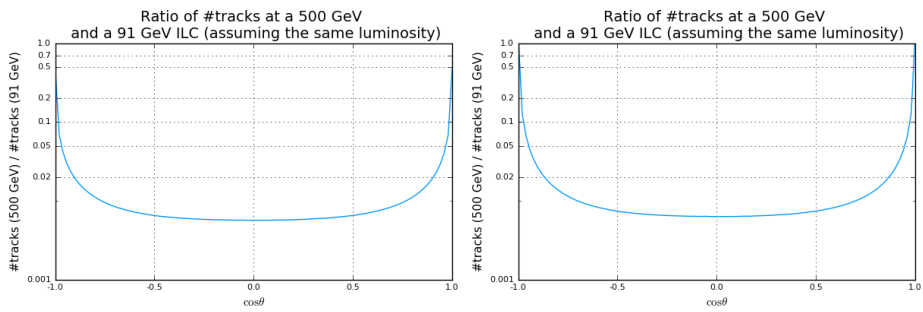
3

Figure 1: Left: Ratio of the number of tracks with energy $p_T > 1$ GeV at 500 GeV vs. at 91 GeV, assuming the same luminosity at both energies. Right: The same plot, but with a cut of 2 GeV.
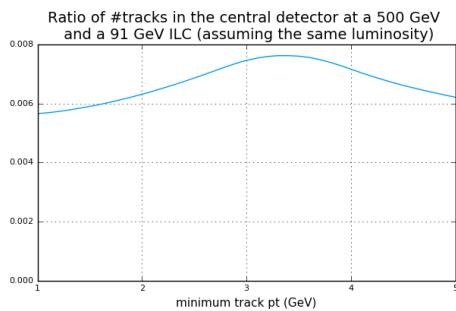

Figure 2: Ratio of the number of tracks at $\theta \approx 90^\circ$ at a 500 GeV ILC and a 91 GeV ILC, as a function of the minimum track p_T.

5   Implications for Alignment

The LHC tracking detectors (e.g. [1]) are able to use tracks to align with sufficient precision that the associated uncertainty is significantly lower than the intrinsic detector resolution. These procedures are carried out with datasets of $\mathcal{O}(10^7)$ high-quality, high-momentum isolated tracks, corresponding to $\mathcal{O}(10^4)$ tracks incident on a given tracking module.

For the ILC, we assume the luminosity ramping scenario from the H-20 scenario [3], with a peak design luminosity of 2×10^{34}, and a beam time of 1.6×10^7 s/year, over an 8 month period. For the first year, it is assumed that the luminosity will ramp up and average 10% of the design value, corresponding to 28 fb^{-1} in the first year, or 3.5fb^{-1}. At 500 GeV, this corresponds to 2.8×10^7 tracks, of which 13% are in the barrel ($|\cos\theta| < 0.625$, $p_T > 2$ GeV), or 3.6×10^6. There are 102×35 modules in the outer layer of SiD, so one would get $\mathcal{O}(10^3)$ tracks in total per module per month at 500 GeV running in the first year.

It is clear that the raw statistical power of track-based alignment at the ILC will be considerably less than that at the LHC, particularly if stringent quality requirements are necessary, and if the procedure has to be repeated between each push-pull operation. An integrated approach to alignment must therefore be taken, which will incorporate specific detector design features, survey and metrology, real-time monitoring (during all phases including beam operation, push-pull movement and garage work), and the maximum use of physics data. The use of beam halo and cosmic rays muons should also be explored (possibly with dedicated electronics operation modes to increase the duty cycle) since tracks not originating from the interaction point are extremely useful in constraining so-called "weak modes".

6   Conclusions on Z-Pole Running

The statistical precision of the data-driven calibration and alignment of detector components at the ILC is likely to be dominated by the incident charged particle flux. At high energies this flux is larger (for a given luminosity) in the forward regions than at the Z-pole. In the barrel region the charged particle flux at high energy is lower than that for the same luminosity at the Z-pole by a considerable factor, but even requiring $p_T > 2$ GeV this factor is not significantly above 100.

The likely instantaneous luminosity available at the Z-pole will be a factor of ≈ 100 less than that at 500 GeV. The statistical power of track alignment and calibration at high energy will therefore be greater than an equivalent time running at the Z-pole, even close to $z = 0$ in the outermost tracking layer.

Running for short periods at the Z-pole will incur not only direct sacrifice of high-energy data taking, but also probable loss of running time due to extra setup periods. There may also be considerable extra costs. There must therefore be a clear and significant physics gain, which is not seen in this study.

This is a preliminary study, and a definitive answer will require more understanding of the alignment and calibration algorithms. However, unless the Z-pole luminosity is considerably greater than the expected 1% of that at 500 GeV, our conclusion is that Z-pole running will have a negative impact on the ILC physics programme. The SiD collaboration therefore requests running only at high energy.

Table 2: List of processes considered at 91 GeV. The weight is the number of events / fb at a 91 GeV ILC running with a beam polarization of $P(e^-)/P(e^+)$ = (-80%/+30%)

Process	#events	polarized XS (fb)	weight/event	#tracks/event	2 GeV, central
2f_qq	10000000	6.055e+07	6.055	21.32	5.85

A List of processes

Table 3: List of processes considered at 500 GeV. The weight is the number of events / fb at a 500 GeV ILC running with a beam polarization of $P(e^-)/P(e^+)$ = (-80%/+30%)

Process	#events	polarized XS (fb)	weight per event	#tracks per event	$p_T > 2$ GeV $|\cos\theta| < 0.7$
2f_z_bhabhag	6468122	3.376e+03	0.001	2.000	0.297
2f_z_h	25233346	1.963e+04	0.001	24.899	4.535
2f_z_l	4946248	3.397e+03	0.001	2.306	0.855
2f_z_vg	7633293	8.498e+03	0.001	0.000	0.000
4f_sw_l	1406516	1.620e+03	0.001	2.161	0.565
4f_sw_sl	4184899	4.853e+03	0.001	20.541	4.003
4f_sze_l	12414037	7.151e+03	0.001	4.106	0.357
4f_sze_sl	3168534	1.883e+03	0.001	16.094	1.206
4f_szeorsw_l	676528	6.520e+02	0.001	2.000	0.579
4f_sznu_l	146826	1.636e+02	0.001	2.180	0.705
4f_sznu_sl	397028	5.588e+02	0.001	20.743	5.361
4f_ww_h	3335134	4.494e+03	0.001	39.337	6.224
4f_ww_l	245713	4.627e+02	0.002	2.324	0.468
4f_ww_sl	4357184	5.570e+03	0.001	20.831	3.297
4f_zz_h	361809	4.074e+02	0.001	42.380	8.630
4f_zz_l	48429	3.640e+01	0.001	3.495	1.024
4f_zz_sl	275931	3.661e+02	0.001	22.604	4.409
4f_zzorww_h	2968283	3.747e+03	0.001	39.372	6.275
4f_zzorww_l	419425	4.803e+02	0.001	2.320	0.474
aa_ee	75977665	7.165e+05	0.009	4.000	0.808
aa_eeee	40004	6.214e+00	0.000	5.999	1.247
aa_eell	40294	3.042e+01	0.001	6.311	1.156
aa_eevv	40004	1.566e+00	0.000	3.999	1.080
aa_eexx	40003	8.859e+00	0.000	14.790	1.370
aa_eeyy	40002	1.276e+00	0.000	16.779	1.945
aa_elvv	40004	2.931e+00	0.000	4.157	1.191
aa_evxy	40002	8.861e+00	0.000	21.868	4.524
aa_levv	40004	2.936e+00	0.000	4.160	1.200
aa_ll	53988976	1.404e+06	0.026	4.316	0.604
aa_llll	40004	2.412e+01	0.001	6.624	1.028
aa_llvv	40004	6.052e+00	0.000	4.323	1.209
aa_llxx	40004	1.696e+01	0.000	15.083	1.271
aa_llyy	40002	2.436e+00	0.000	16.997	1.854
aa_lvxy	42149	1.770e+01	0.000	22.035	4.591

6

aa_vexy	40004	8.858e+00	0.000	21.838	4.508
aa_vlxy	42146	1.770e+01	0.000	21.970	4.588
aa_vvxx	40003	1.276e-01	0.000	15.926	1.277
aa_vvyy	40004	1.529e-02	0.000	16.215	1.269
aa_xx	21257900	5.091e+05	0.024	12.635	0.440
aa_xxxx	39998	1.477e+00	0.000	25.126	2.019
aa_xxyy	64973	5.119e+01	0.001	39.949	8.153
aa_yy	18380202	4.774e+04	0.003	12.972	0.404
aa_yyyy	40002	4.277e-02	0.000	32.418	3.982
aamin_04_10_m1	400147	3.876e+03	0.010	34.274	0.028
aamin_04_10_m4	400030	7.373e+04	0.184	27.850	0.121
aamin_10_20_m1	400140	6.250e+02	0.002	40.346	0.367
aamin_10_20_m4	400032	5.158e+03	0.013	30.703	0.807
aamin_20_40_m1	400148	1.626e+02	0.000	43.774	1.977
aamin_20_40_m4	400025	8.147e+02	0.002	32.998	2.570
aamin_40_xx_m1	400152	3.282e+01	0.000	45.357	5.548
aamin_40_xx_m4	400033	1.076e+02	0.000	35.637	5.607
ae_eee	61686424	3.173e+04	0.001	4.000	0.768
ae_ell	60725620	6.705e+04	0.001	4.330	0.618
ae_evv	2134181	1.234e+03	0.001	2.000	0.525
ae_exx	19182844	2.399e+04	0.001	13.703	1.288
ae_eyy	7857137	4.028e+03	0.001	17.213	1.453
ae_lvv	1676981	1.090e+03	0.001	2.161	0.616
ae_vxy	4954353	3.220e+03	0.001	20.170	4.384
bbcyyc	886	2.235e+00	0.003	65.573	22.743
ea_eee	61684156	3.173e+04	0.001	4.000	0.767
ea_ell	60729341	6.705e+04	0.001	4.330	0.618
ea_evv	2132912	1.512e+03	0.001	2.000	0.526
ea_exx	19182117	2.413e+04	0.001	13.705	1.288
ea_eyy	7850151	4.191e+03	0.001	17.220	1.455
ea_lvv	1675377	1.508e+03	0.001	2.162	0.617
ea_vxy	4952472	4.457e+03	0.001	20.167	4.392
eeeeee	40004	3.337e-02	0.000	5.999	1.130
eeeell	10001	1.252e-02	0.000	6.344	1.027
eeveev	30003	3.938e-01	0.000	3.999	1.398
eevelv	10001	1.295e-01	0.000	4.163	1.465
eevlev	10001	5.872e-01	0.000	4.154	1.643
eevllv	10001	1.416e+00	0.000	4.320	1.733
llvelv	20002	3.705e-01	0.000	4.480	2.234
llvllv	20002	6.238e-01	0.000	4.644	2.113
neu1neu2g	23547	4.631e+01	0.002	0.258	0.000
vvveev	10001	2.136e-03	0.000	2.000	0.618
vvvelv	10001	5.388e-01	0.000	2.162	1.080
vvvlev	10001	2.501e-04	0.000	2.166	1.491
vvvllv	20002	1.031e+00	0.000	2.327	1.210
xxxyyx	1115	9.183e+00	0.008	59.074	16.603
yycyyu	203	2.238e+00	0.011	63.783	22.522
yyuyyc	427	2.247e+00	0.005	64.998	22.459
yyvllv	5798	4.711e+01	0.008	28.771	10.594

Total	3.096e+06	6.87

References

[1] Alignment of the CMS tracker with LHC and cosmic ray data, The CMS Collaboration, JINST 9 (2014) P06009

[2] ILC possibilities at Z and W `http://ilcdoc.linearcollider.org/record/63004/files/ILC\%20possibilities\%20at\%20Z\%20and\%20W.pdf`

[3] T. Barklow, J. Brau, K. Fujii, J. Gao, J. List, N. Walker and K. Yokoya, "ILC Operating Scenarios", arXiv:1506.07830 [hep-ex].